Electrochimica Acta 146 (2014) 845–849

Contents lists available at ScienceDirect

Electrochimica Acta

journal homepage: www.elsevier.com/locate/electacta

Effect of Series and Shunt Resistance on Organic-Inorganic Hybrid Solar Cells Performance

Jie Zhang, Shuit-Tong Lee, Baoquan Sun*

Jiangsu Key Laboratory for Carbon-Based Functional Materials and Devices, Institute of Functional Nano and Soft Materials (FUNSOM), Soochow University, Suzhou 215123, Jiangsu, China

ARTICLE INFO

Article history:
Received 3 June 2014
Received in revised form 14 August 2014
Accepted 14 August 2014
Available online 6 September 2014

Keywords:
Hybrid Organic-inorganic Solar Cells
Duodiode Model
Shunt Resistance
Series Resistance

ABSTRACT

Organic-inorganic solar cells based on n-type silicon (100) and poly (3,4-ethylenedioxythiophene): poly(styrenesulfonate) (PEDOT:PSS) exhibit great photo-electron conversion abilities while utilizing a simple fabrication process. In organic-inorganic hybrid solar cells, the device can be described by an equivalent circuit for a duodiode model. In this model, it is found that the fluctuation of the series and shunt resistance can dramatically influence the output characteristics. In this letter, the series and shunt resistance is tuned to observe its effect on the device performance. It is found that with suitable substrate scales and physical tailoring methods, the shunt and series resistances can be adjusted to eliminate the unfavorable charge trapping phenomenon. Meanwhile, the fill factor is also enhanced notably up to 0.74, which yields a power conversion efficiency of 12.1%. These results indicate that the junction quality plays a key role in the performance of the hybrid organic-inorganic solar cell.

1. Introduction

Conventional inorganic crystalline silicon (c-Si) solar cells are mainly limited by high-cost fabrication processes and expensive materials, although they come with great benefits, such as large power conversion efficiency (PCE), amount of available source material and good fabrication processes. A traditional p-n junction is usually produced under high temperature diffusion, requiring elaborate equipments [1,2]. On the other hand, organic-inorganic hybrid heterojunction solar cells are promising candidates for low-cost energy converters [3–5]. Among them, poly(3, 4-ethylenedioxythiophene):polystyrenesulfonate (PEDOT:PSS) has attracted wide attentions for its high electric conductivity, transparency and solution-processed properties [6–10]. Many studies have demonstrated PEDOT:PSS and c-Si hybrid structured solar cells, e.g. using silicon nanowire arrays (SiNWs) with efficient light trapping and harvesting, SiNWs/PEDOT:PSS core/shell nanowire array heterojunction solar cells achieve an efficiency of greater than 11% [5,11–15]. Organic-inorganic hybrid devices consist of a Schottky junction between n-Si and PEDOT:PSS as well as a rear electrode. The PEDOT:PSS film acts as a window electrode, which allows light to reach Si. This film shows good light transparency (>90%, 300-1100 nm) with high conductivity (up to 1000 S•cm^{-1}). In order to improve the hole collection efficiency, a silver grid electrode was deposited onto the PEDOT:PSS layer. PEDOT:PSS with a work function of ~5.1 eV was used for hole collection and a rear metal electrode was used for electron collection. Light was harvested by the Si substrate and a depletion layer was formed within Si to sweep the charges toward their proper respective directions.

It is known that both the open circuit voltage (V_{oc}) and fill factor *(FF)* of the photovoltaic device influence the PCE besides short circuit current density (J_{sc}). The upper limit on V_{oc} is determined by carrier recombination in the bulk of silicon, if we can assume that the interfacial recombination is negligible. In order to improve the J_{sc} for the PEDOT:PSS/Si hybrid solar cell, SiNWs have been used in order to enhance their light harvesting capability. A device with a J_{sc} value as high as 34.5 mA/cm^2 has been realized through the use of hierarchical Si surfaces consisting of micropyramids and nanowires [5].

Besides J_{sc}, the *FF* is also a quantity of interest in the achievement of a high PCE hybrid solar cell. In this work, the series and shunt resistances are optimized to achieve an enhanced *FF*. In this organic-inorganic hybrid solar cell, it can be described by an equivalent circuit for a duodiode model. In this model, it is found that the fluctuation of the series and shunt resistance can dramatically influence output characteristics. The optimized device displays an excellent PCE of 12.1% under a simulated air mass (AM) 1.5 at 100 mW/cm^2. It was found that with suitable substrate scales and

* Corresponding author. Tel.: +86 512 65880820; fax: +86 512 65882846.
E-mail address: bqsun@suda.edu.cn (B. Sun).

http://dx.doi.org/10.1016/j.electacta.2014.08.065
0013-4686/

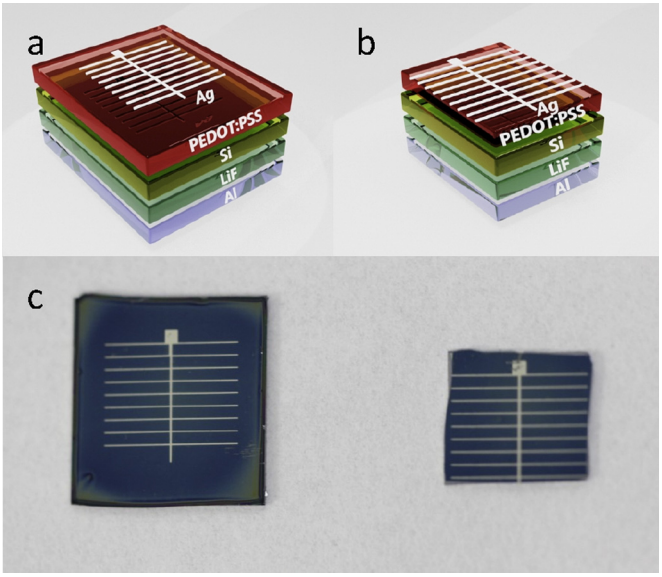

Fig. 1. Device structure of the planar Si/PEDOT heterojunction hybrid solar cell (a) before using the physical tailoring method, (b) after using the physical tailoring method, (c) optical images of the devices.

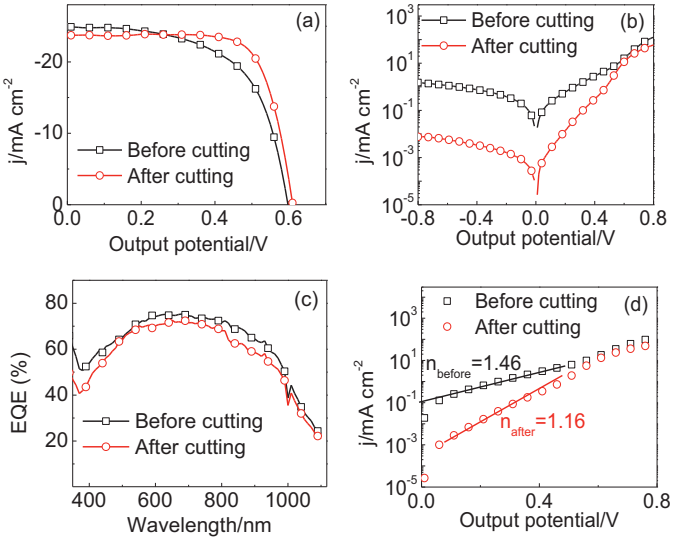

Fig. 2. Electric output characteristics of devices based on various silicon substrate scales. (a) *J–V* curves of the devices under the simulated illumination of AM 1.5 at 100 mW/cm^2. (b) *J–V* curves of the devices under dark condition. (c) EQE spectra of the devices versus wavelength. (d) *J–V* curves of the devices under dark condition deducing the diode ideality factors.

physical tailoring methods, the shunt and series resistances can be adjusted, resulting in great performance enhancement of the hybrid organic-inorganic solar cell.

2. Experiment

An n-type Si (100) wafer (of resistivity 5 Ω·cm) was sequentially cleaned in acetone; ethanol and deionized (DI) water for 20 minutes each at room temperature and then cleaned in concentrated H_2SO_4 and H_2O_2 blends for 1 hour at 110 °C. The silicon substrate was methylated and a PEDOT:PSS (PH1000, Clevios) film was deposited on the planar silicon substrate by the process of spin coating. The substrate was annealed at 115 °C in an ambient environment. 200 nm thick silver grid contacts were deposited on top of the PEDOT:PSS film through electron beam evaporation [16]. This metal portion covered 10% of the top surface area. Finally, 0.5 nm LiF and 200 nm Al were deposited on the back of the Si substrate through thermal evaporation. More detailed information is concluded in supporting information.

Using physical tailoring methods, that is to cut the spare area of substrate with diamond knife, leaving area only with silver grid, substrate scales were adjusted into suitable ones and higher performances were obtained. Device structure of the planar PEDOT:PSS/Si heterojunction hybrid solar cell and optical images of the devices are shown in Fig. 1. The whole area before cutting the substrate is about 1.5 × 1.5 cm^2 and after the physical tailoring methods is applied, the area is modified into 1.0 × 0.9 cm^2. The solar simulator Newport 91160 was equipped as an incoming light source to produce the simulated solar spectra. The light intensity was 100 mW•cm^{-2}, which was adjusted using a standard silicon photovoltaic device (91150, Newport). The C^{-2}-*V* curves are yielded by a Wayne Kerr 6500B.

3. Results and Discussion

The current-voltage (*J–V*) curves of the device before and after the physical tailoring method was applied on the Si substrate are plotted in Fig. 2.

The device based on PEDOT:PSS/Si exhibited a J_{sc} of 24.9 mA/cm^2, an open circuit voltage (V_{oc}) of 0.59 V, a *FF* of 0.61, a series resistance of 2.75 Ω•cm^2 and a shunt resistance of 316.1 Ω•cm^2, yielding a PCE of 8.9%. The physical tailoring method was then immediately applied on the Si substrate to reduce the substrate size. After this operation, the device displayed a J_{sc} of 23.7 mA/cm^2, a V_{oc} of 0.61 V, a *FF* of 0.74, a series resistance of 0.91 Ω•cm^2 and a shunt resistance of 344.3 Ω•cm^2, achieving a PCE of 10.7%. This method can greatly improve device performance, especially the *FF* which exhibited more than 20% enhancement. The electric output characteristics are summarized in Table 1. The areas used to calculate the J_{sc} before and after the cutting step is 0.8 cm^2. The whole area of substrate before being cut is about 1.5 × 1.5 cm^2, the large area of the Si substrate can ensure an uniform PEDOT:PSS film when PEDOT:PSS was spincoated on Si substrate than a relative small substrate. The hollow area of shadow mask for the measurement is 0.8 × 1.0 cm^2 in order to give an accurate device area which is in agreement with Ag grid area; the shape of the shadow mask is plotted in supporting information. So part of the solar cell which is not shined under the incoming light source will not work as the solar cell but only as resistance. Those resistances will deteriorate the power conversion ability, and after they are removed by physical tailoring method, which means resistance is eliminated significantly, the FF is greatly increased; the quality of Schottky junction is developed; and the performance is actually improved correspondingly. The dark current was greatly suppressed after the physical tailoring method, as shown in Fig. 2**(b)**. The saturation current density (J_s) was suppressed significantly from 9.0 × 10^{-6} mA/cm^2 to 3.4 × 10^{-7} mA/cm^2. The J_s values were extracted from the dark J-V curves according to the thermionic emission model. A lower J_s suggests a relatively higher V_{oc}. A smaller series resistance and a larger shunt resistance leads to a higher *FF* [17], which is consistent with our observation. The device after edge cutting displayed dramatic *FF* improvement as well as slight V_{oc} enhancement. The dark current *versus* voltage curves plotted in Fig. 2**(d)** display an improved diode ideality factor (n) from 1.46 (before) to 1.16 (after), indicating that less charge recombination currents within both interface and bulk charge region after application of the physical tailoring method, resulting from reduction of defect states and improvement of Schottky junction quality [18,19]. The ideality factor of a diode is a measure of how closely the diode follows the ideal diode equation. If the

Table 1
The electronic output characteristics of organic-inorganic heterojunction photovoltaic devices based on various silicon substrate scales. The device is preserved in air for 4 h.

Devices Group	V_{oc} (V)	J_{sc} (mA/cm^2)	FF	PCE (%)	R_s (Ω•cm^2)	R_{sh} (Ω•cm^2)
Before cutting	0.59	24.9	0.61	8.9	2.75	316.1
After cutting	0.61	23.7	0.74	10.7	0.91	344.3
4 h later	0.61	27.1	0.73	12.1	0.4	367.2

recombination is limited by minority carrier, the ideality factor will be 1; otherwise, if the recombination is limited by both carriers, then it will be 2. External quantum efficiency (EQE) was plotted for the devices before and after the substrate scales were changed. The EQE spectra gave similar profiles after the Si substrate was modified, which is consistent with the values of J_{sc} before and after substrate modification.

Fig. 3 **(a)** shows the energy band diagram of the PEDOT:PSS/Si Schottky junction. A is constant-current source, I_L is the current value of the constant-current source, I_{D1} is the current value of diode D1 with ideal factor 1 and I_{D2} is the current value of diode D2 with ideal factor 2, I_{RP} is the current value of shunt resistance R_{sh}. The Schottky barrier height (Φ_B) can be expressed as $\Phi_B = V_{bi} + kT\bullet\ln(N_C/N_D)/q$ [20]. Here V_{bi} is the built-in voltage, N_C is the effective density of states in the conduction band, and N_D is the doping concentration of the semiconductor. Based on an ideal Schottky-Mott model, Φ_B corresponds to the difference between the work function (W_P) and electron affinity of Si (χ_S) in an ideal condition, giving $q\Phi_B = W_P - \chi_{Si}$. Fig. 3 **(b)** exhibits C^{-2}-V plots of devices based on different silicon substrates. The value of V_{bi} can be deduced from the curves of the capacitance-voltage (C^{-2}–V) characteristics. As we know, both interface defect states and bulk defect states were distributed in the silicon solar cell; after the device area is reduced the corresponding defect states are cut down, and less charge recombination will happen. So more charge carriers will not recombine but will drift to Si and the PEDOT:PSS film zone, respectively. Hence the built-in electric field is enhanced and the V_{bi} is enlarged, corresponding to the enhancement of V_{oc}. The improvement of V_{oc} is the conclusion come from the analysis of Schottky-Mott model.

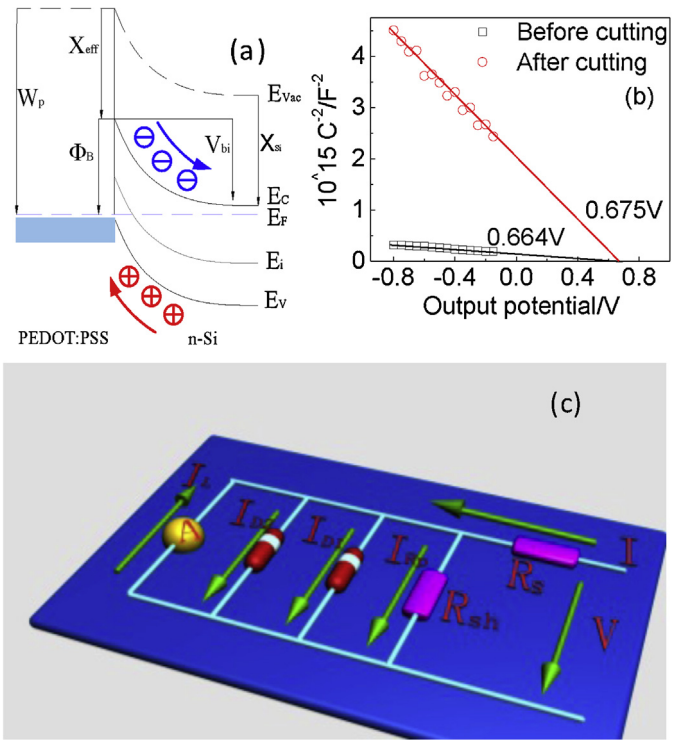

Fig. 3. (a) Energy band diagram of the PEDOT:PSS/Si Schottky junction. (b) C^{-2}-V plots of devices based on different silicon substrates, the data are recorded at a frequency of 100 Hz. (c) Equivalent circuits for duodiode model.

It was calculated from the curves that V_{bi} before and after substrate modification were 0.664 V and 0.675 V, respectively, corresponding to the small enhancement of V_{oc}, resulting from an improved *FF*. As we know, there exist bulk defect states in Si; after the device area is reduced and less charge recombination will happen. However, under the same light irradiation, the charge concentration should not change, so more holes and electrons will drift to Si and the PEDOT:PSS film zone. Hence the built-in electric field is enhanced and the V_{bi} is enlarged. In a real situation there always exists series and shunt resistance. Fig. 3 **(c)** shows the equivalent circuit for a duodiode model [21,22]. For the case that the shunt resistance is too large to be considered in the equivalent circuit for the duodiode model, but the series resistance is important, the *FF* can be expressed by $FF = FF_0(1-r_s)$, where FF_0 is the ideal *FF*, and can be expressed as

$$FF_0 = \frac{v_{oc} - \ln(v_{oc} + 0.72)}{v_{oc} + 1}$$

Here $v_{oc} = V_{oc}/(nkT/q)$. r_s in the expression for *FF* is the normalized series resistance given by $r_s = R_s/R_{CH}$, where R_s is the series resistance and R_{CH} is the characteristic resistance given by $R_{CH} = V_{oc}/I_{sc}$. Based on these equations, before the device area was modified, FF_0 was calculated to be 0.77, r_s to be 0.116, and *FF* to be 0.68. After the device area was modified to be smaller, FF_0 was calculated to be 0.81, r_s to be 0.035, and *FF* to be 0.78. This can be seen from theory: a small series resistance can lead to an improved *FF* [17,23,24]. In the case where the series resistance is negligibly small but the shunt resistance is important, the *FF* can be expressed as $FF = FF_0(1-1/r_{sh})$, where $r_{sh} = R_{sh}/R_{CH}$ is the normalized shunt resistance; here R_{sh} is the shunt resistance [23,24]. For this case, before the device area was modified, r_{sh} was calculated to be 13.34, and *FF* to be 0.71. After the device area was modified to be smaller, r_{sh} was calculated to be 13.38, and *FF* to be 0.75. This can also be easily seen from theory; a large shunt resistance will give a better *FF*. For the case in which both shunt and series resistances are important, the expression for *FF* contains terms relating to both these quantities, giving $FF = FF_0(1-r_s)\bullet(1-1/r_{sh})$. Using this expression, we calculate the *FF* before device modification to be 0.62 and after modification to be 0.72. The measured *FF* for these two cases was found to be 0.61 and 0.74 respectively, which are very close to what we have deduced from the equations above, suggesting that the equivalent circuit for the duodiode model is quite coincident with the device structure and that the calculations for *FF* are accurate in this organic-inorganic hybrid Schottky junction device. The *FF* is used as a measure of solar cell quality (influenced by both shunt and series resistances), and is a measure of the maximum possible power area contained within the solar cell *J-V* characteristic curve with the ideal power area corresponding to the values of V_{oc} and J_{sc}. *FF* is defined as the maximum output power divided by the ideal output power. Based on this calculation and the analysis above, *FF* should ideally be 1; however, the features of the organic-inorganic hybrid Schottky junction should not allow it to reach 1. A larger value of *FF* indicates a higher quality of the solar cell. Normally, the *FF* is around 60~80% and is strongly influenced by the materials and device structure of the solar cell. In order to obtain a

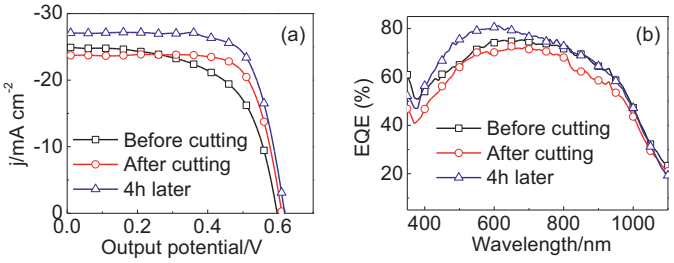

Fig. 4. (a) Electric output characteristics of devices based on various silicon substrate scales and (b) EQE spectra of the devices versus wavelength.

high efficiency solar cell, the *FF* must be high, the reverse saturated dark current should be low, the ideal factor should be close to 1, the shunt resistance must be high and the series resistance must be low.

After the device was placed in ambient conditions for 4 hours, it was found that with almost steady V_{oc} and *FF*, the J_{sc} dramatically improved from 23.7 mA/cm^2 to 27.1 mA/cm^2, leading to an enhancement of the PCE from 10.7% to 12.1%. Electric output characteristics and EQE spectra of the devices versus wavelength are presented in Fig. 4. The electronic output characteristics of organic-inorganic heterojunction photovoltaic devices based on various silicon substrate scales and time-dependence variation are summarized in Table 1. After the physical tailoring method was applied and the device was placed in air, PEDOT:PSS film was generally oxidized and film resistance was suppressed from 220 Ω·cm/□ to 177 Ω·cm/□, leading to a depressed series resistance and an improved shunt resistance consequently, resulting in a better J_{sc}. The highest PCE of a device exposure in air for 4 h is an optimized result. If the device is continuously exposure in air, the performance will be deteriorated; the results are shown in supporting information. However, if the device is preserved in inner circumstance, the device performance remains almost unchanged, suggesting a good stability of device performance.

Simulation work is also researched and exhibited here to give support for the effect of series and shunt resistance on the solar cells performance. The simulation tool and method are discussed in supporting information. In Fig. 5, simulation illustrations for electric output characteristics of devices based on (a) various series resistances, and (b) various shunt resistances. In Fig. 5 **(a)**, as series resistance decreases from 10 Ω•cm^2 to 0.1 Ω•cm^2, the *FF* is improved dramatically from 0.35 to 0.82; meanwhile, in Fig. 5 **(b),** as shunt resistance increases from 10 Ω•cm^2 to 1000 Ω•cm^2, the *FF* is enhanced from 0.25 to 0.82, which is highly corresponding to the discussed results above. The *FF* is influenced strongly by both the shunt and the series resistances, as the analysis and calculation data above, the larger value of *FF* will lead to a better quality of solar cell. The simulated high *FF* is around 80%, which is also very close to the discussion before. These simulation results can confirm that both the shunt and the series resistances are very important

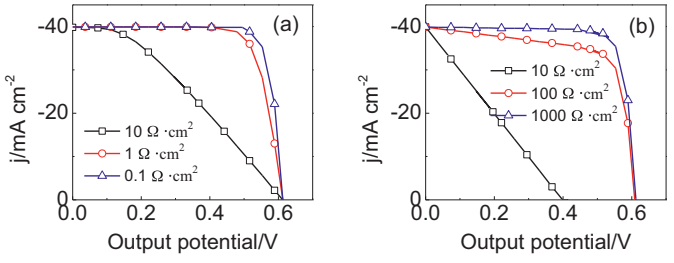

Fig. 5. Simulation illustrations for electric output characteristics of devices based on (a) various series resistances, and (b) various shunt resistances.

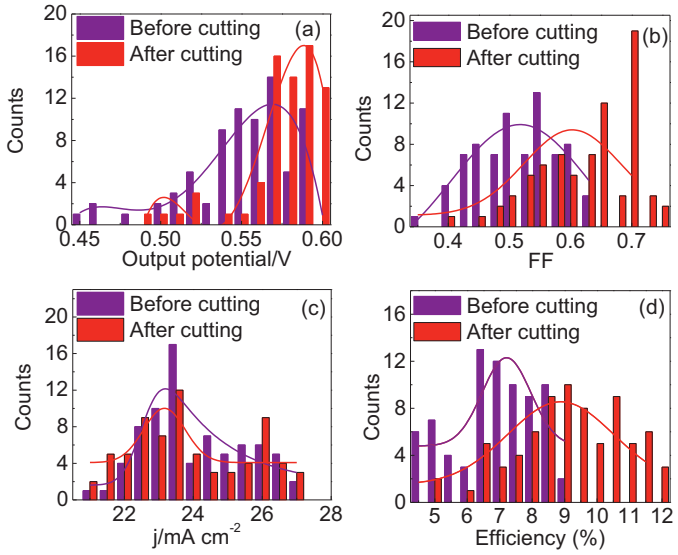

Fig. 6. A histogram for each value of (a) V_{oc}, (b) *FF*, (c) J_{sc}, and (d) PCE of 78 samples.

to solar cell performance as the *FF* is strongly influenced by them [25].

In order to check the reproducibility of this physical tailoring method, fabrication of the devices was repeated. As shown in Fig. 6, a histogram for each value of the V_{oc}, the *FF*, the J_{sc}, and the PCE of 78 samples was plotted. Almost all devices had improved *FF*, small enhancement of the V_{oc}, steady J_{sc}, and better PCE after the physical tailoring method was applied on them, indicating that this method is a highly effective way to improve the performance of all devices. The peak of the V_{oc} distribution shifts from about 0.57 V to around 0.59 V before and after applying this method. The *FF* significantly improved such that the distribution was enhanced almost 20% from 0.5 to 0.6 and some even achieved a value of around 0.7. The J_{sc} distribution shares nearly the same profile for there is no obvious difference in the process. All these distributions indicate an improved PCE; most devices show better performance, which is coincident with the analysis discussed above.

4. Conclusion

In summary, hybrid organic-inorganic solar cells based on n-type silicon (100) and PEDOT:PSS exhibit photo-electron conversion abilities (12.1%) along with a simple fabrication process under AM 1.5G illumination at 100 mW/cm^2. An equivalent circuit for a duodiode model is raised to describe the solar cell. In this model, the fluctuation of the series and shunt resistance can dramatically influence the output characteristics. It is investigated that with proper substrate scales and physical tailoring methods, the shunt and series resistances can be adjusted to eliminate the unfavorable charge trapping phenomenon, resulting in great performance enhancement of the hybrid organic-inorganic solar cell. This simple method can be used to improve hybrid solar cell performance greatly.

Acknowledgement

This work was supported by the National Basic Research Program of China (973 Program) (2012CB932402), the National Natural Science Foundation of China (91123005, 61176057, 61211130358), the Priority Academic Program Development of Jiangsu Higher Education Institutions.

Appendix A. Supplementary data

Supplementary data associated with this article can be found, in the online version, at http://dx.doi.org/10.1016/j.electacta.2014.08.065.

References

[1] J. Zhao, A. Wang, M.A. Green, F. Ferrazza, Appl. Phys. Lett. 73 (1998) 1991.
[2] J. Zhao, A. Wang, P.P. Altermatt, S.R. Wenham, M.A. Green, Sol. Ener. Mater. Sol. Cells 41 (1996) 87.
[3] F. Zhang, D. Liu, Y. Zhang, H. Wei, T. Song, B. Sun, ACS Appl. Mater. Interfaces 5 (2013) 4678.
[4] L. He, D. Lai, H. Wang, C. Jiang, Rusli, Small 8 (2012) 1664.
[5] W.R. Wei, M.L. Tsai, S.T. Ho, S.H. Tai, C.R. Ho, S.H. Tsai, C.W. Liu, R.J. Chung, J.H. He, Nano Lett. 13 (2013) 3658.
[6] C. Tengstedt, A. Crispin, C. Hsu, C. Zhang, I. Parker, W. Salaneck, M. Fahlman, Org. Electron. 6 (2005) 21.
[7] H.W. Heuer, R. Wehrmann, S. Kirchmeyer, Adv. Funct. Mater. 12 (2002) 89.
[8] J. Ouyang, C.-W. Chun, F.-E. Chen, Q. Xu, Y. Yang, Adv. Funct. Mater. 15 (2005) 203.
[9] X. Crispin, F.L.E. Jakobsson, A. Crispin, P.C.M. Grim, P. Andersson, A. Volodin, C. van Haesendonck, M. Van der Auweraer, W.R. Salaneck, M. Berggren, Chem. Mater. 18 (2006) 4354.
[10] R. Kiebooms, A. Aleshin, K. Hutchison, F. Wudl, A. Heeger, Synthetic Metals 101 (1999) 436.
[11] W. Lu, C. Wang, W. Yue, L. Chen, Nanoscale 3 (2011) 3631.
[12] S.C. Shiu, J.J. Chao, S.C. Hung, C.L. Yeh, C.F. Lin, Chem. Mater. 22 (2010) 3108.
[13] B. Ozdemir, M. Kulakci, R. Turan, H. Emrah Unalan, Appl. Phys. Lett. 99 (2011) 113510.
[14] X. Shen, D. Liu, S. Lee, B. Sun, J. Am. Chem. Soc 133 (2011) 19408.
[15] J. Zhang, Y. Zhang, F. Zhang, B. Sun, Appl. Phys. Lett. 102 (2013) 013501.
[16] O. Gunawan, S. Guha, Sol. Ener. Mater. Sol. Cells 93 (2009) 1388.
[17] K. Rmkanans, J. Sheechun, Solid-State Electronics 22 (1987) 193.
[18] F. Zhang, X. Han, S. Lee, B. Sun, J. Mater. Chem. 22 (2012) 5362.
[19] N. Jensen, U. Rau, R.M. Hausner, S. Uppal, L. Oberbeck, R.B. Bergmann, J.H. Werner, J. Appl. Phys. 87 (2000) 2639.
[20] S.M. Sze, Semiconductor Devices: Physics and Technology., Wiley, 2008.
[21] S. Silvestre, A. Chouder, Prog. Photovoltaics 16 (2008) 141.
[22] P.P. Altermat, G. Heiser, M.A. Green, Prog. Photovoltaics 4 (1996) 355.
[23] M.A. Green, Solid-State Electronics 24 (1981) 788.
[24] M.A. Green, Solar Cells 7 (1982) 37.
[25] R. Kuhn, P. Fath, E. Bucher, in Conference Record of the Twenty-Eighth IEEE Photovoltaic Specialists Conference (2000) 116.